Plasmonics (2011) 6:311–317
DOI 10.1007/s11468-011-9206-7

Refractive Index Sensitivity Analysis of Ag, Au, and Cu Nanoparticles

Jagmeet Singh Sekhon · S S Verma

Received: 8 November 2010 / Accepted: 13 January 2011 / Published online: 27 January 2011

Abstract The localized surface plasmon resonance (LSPR) spectrum of noble metal nanoparticles is studied by quasi-static approximation. Taking the sensitivity of LSPR shape to the size and shape of nanoparticle along with surrounding refractive index, parameters like refractive index sensitivity and sensing figure of merit have been determined. In the present analysis from the sensing relevant parameters, it is concluded that Ag represents a better sensing behavior than Au and Cu over the entire visible to infrared regime of EM spectrum.

Keywords Localized surface plasmon resonance · Prolate · Nanosphere · Plasmonics · Sensing figure of merit

Introduction

Novel metal nanoparticle (much smaller than the wavelength of light) shows remarkable optical properties due to collective excitation of conduction electrons [1]. Light incident on the nanoparticle induces the conduction electrons to oscillate collectively with a resonant frequency/wavelength called localized surface plasmon resonance (LSPR) frequency/wavelength. The shape of the nanoparticle extinction spectra, i.e., the LSPR wavelength (λ_{max}), and resonant line width (full width half maxima, FWHM) depend on nanoparticle material, size, shape, and surrounding medium refractive index [2–5]. Support LSPR varied over the entire visible to infrared region of EM spectrum. The LSPR wavelength generally shifts toward higher wavelength as the refractive index of surrounding medium increases. This LSPR wavelength dependence on the surrounding refractive index forms the basis of plasmonic bio/chemical sensors [1, 4–10].

Au nanoparticles are most commonly used due to their high stability and easy fabrication, but recently other plasmonic material nanoparticles, viz., Ag and Cu have also attracted considerable attention for plasmonic sensing [4–11]. These materials have absorbing oxide layers that strongly dampen the LSPR, which must be removed by glacial acetic acid to restore a narrow resonance line width [11]. The refractive index sensitivity (S) of nanoparticles is a key factor in determining their usefulness for bio/chemo sensors. Further improvement in the index sensitivity of metal nanoparticles requires the identification of critical structural and plasmonic parameters. Since FWHM affects the sensitivity of such type of sensors, therefore, to check their general performance, a figure of merit (FOM) defined as the ratio of refractive index sensitivity (S) to resonant line width has been proposed [5, 10, 12, 13]. Different experimental and theoretical studies [5, 9, 10] have been carried out to optimize the structure and their dimension for optical sensing. Although many experimental studies has been carried out for the synthesization of Ag and Cu nanoparticles [9, 14–17] but as per our knowledge, no work to study the sensing behavior and their optimization for FOM performance has yet been reported.

In the present quasi-static approximation, Mie theory and Gans theory have been used to model the extinction spectrum of Ag, Au, and Cu for their nanosphere and prolate shapes, respectively. The refractive index sensitivity calculations are carried out in order to use these materials in plasmonic sensing applications. Moreover, nanoparticle structure and material optimization are reported from

J. Singh Sekhon (✉) · S. S Verma
Department of Physics, Sant Longowal Institute
of Engineering & Technology,
Longowal, District-Sangrur, Punjab 148-106, India
e-mail: jagmeetsekhon@ymail.com

FOM viewpoint, from visible to infrared region of EM spectrum, and simulated FOM behavior is explained on the basis of quality factor (Q).

Modeling

In the present study, simulations for LSPR are made by using Mie calculations, performed by "MiePlotv4.1" (http://philiplaven.com/MiePlot.htm) for spherical particles. The algorithm of this software is based on the Mie scattering calculations from a sphere. Scattering of light by particles is described by aggregate of materials that constitute a region with refractive index (n_{mat}), which differs from the refractive index of its surrounding medium (n_m). According to Mie calculations [8], scattering and absorption cross sections are expressed as

$$\sigma_{\mathrm{sca}} = \frac{2}{x^2}\sum_{n=1}^{\infty}(2n+1)\left(|a_n|^2+|b_n|^2\right) \tag{1}$$

$$\sigma_{\mathrm{abs}} = \frac{2}{x^2}\sum_{n=1}^{\infty}(2n+1)\left\{\mathrm{Re}\,(a_n)-|a_n|^2+\mathrm{Re}\,(b_n)-|b_n|^2\right\} \tag{2}$$

and the extinction (scattering+absorption) cross section is given by

$$\sigma_{\mathrm{ext}} = \frac{2}{x^2}\sum_{n=1}^{\infty}(2n+1)\,\mathrm{Re}\,(a_n+b_n) \tag{3}$$

where, a_n and b_n are Mie coefficients and are given below

$$a_n = \frac{\psi_n'(n_{\mathrm{mat}}x)\psi_n(x) - n_{\mathrm{mat}}\psi_n(n_{\mathrm{mat}}x)\psi_n'(x)}{\psi_n'(n_{\mathrm{mat}}x)\varsigma_n(x) - n_{\mathrm{mat}}\psi_n(n_{\mathrm{mat}}x)\varsigma_n'(x)} \tag{4}$$

$$b_n = \frac{n_{\mathrm{mat}}\psi_n'(n_{\mathrm{mat}}x)\psi_n(x) - \psi_n(n_{\mathrm{mat}}x)\psi_n'(x)}{n_{\mathrm{mat}}\psi_n'(n_{\mathrm{mat}}x)\varsigma_n(x) - \psi_n(n_{\mathrm{mat}}x)\varsigma_n'(x)}, \tag{5}$$

here, $x=\frac{2\pi r n_{\mathrm{med}}}{\lambda}$, r is the sphere radius, λ is the wavelength of incident light, and ψ and ς are Riccati–Bessel functions. When the size of nanoparticle is much smaller than the wavelength of incident light (in quasi-static approximation), only dipole term (first term) is important in Eq. 3 and

$$\sigma_{\mathrm{ext}} = \frac{2\pi V\varepsilon_m^{\frac{3}{2}}}{3\lambda}\sum_j \frac{\left(\frac{1}{L_j^2}\right)\varepsilon_2}{\left(\varepsilon_1+\frac{1-L_j}{L_j}\varepsilon_m\right)^2+\varepsilon_2^2} \tag{6}$$

where L_i "is an added geometrical factor whose value L_i=1/3" or less than "1/3" for spherical or prolate (depending on the aspect ratio) particles, respectively. The depolarization factor [5, 14] (also called screening parameter) along the long axis of ellipsoid is

$$L_x = \frac{1}{\mathrm{AR}^2-1}\left(\frac{\mathrm{AR}}{2\sqrt{\mathrm{AR}^2-1}}\ln\frac{\mathrm{AR}+\sqrt{\mathrm{AR}^2-1}}{\mathrm{AR}-\sqrt{\mathrm{AR}^2-1}}-1\right) \tag{7}$$

where, "$\mathrm{AR}=\frac{a}{b}$" represents the aspect ratio of prolate. It is clear that the optical properties of nanoparticle depends on the dielectric constant of the medium $\varepsilon_{\mathrm{Au}}(\omega)$, aspect ratio "AR," and surrounding medium dielectric constant ε_m, but not on the size of prolate. The long and short axes of the ellipsoid are represented by a and b, respectively with long axis along X-axis. Thus, to tune the extinction (i.e., absorption and scattering) lines of the prolate, we have changed the aspect ratio and surrounding medium dielectric constant, but not the size.

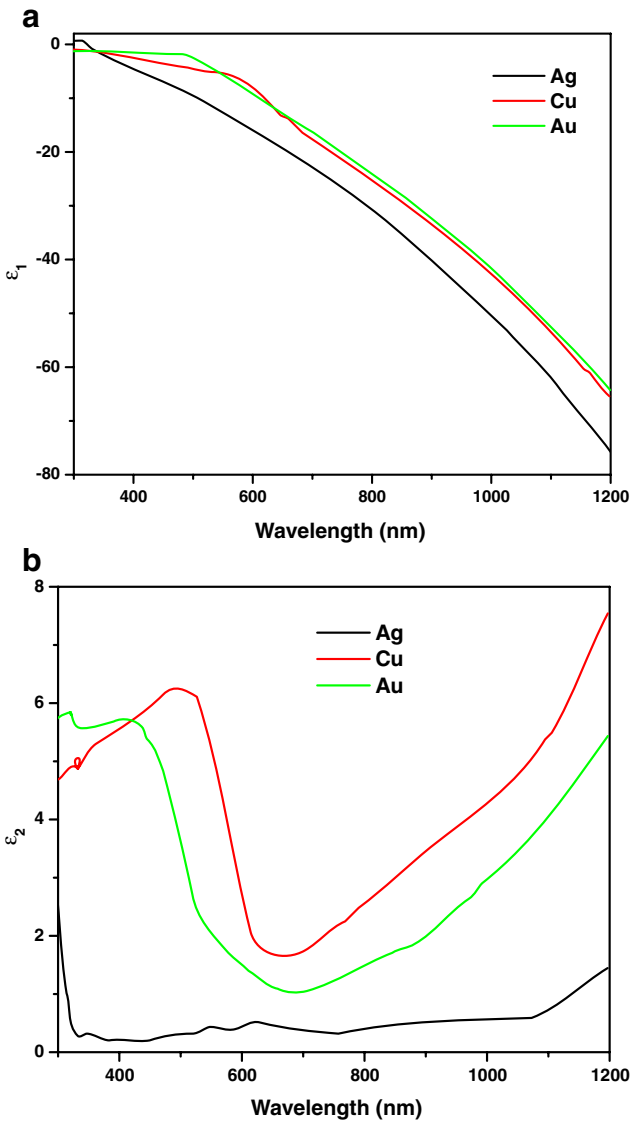

Fig. 1 Dielectric constant comparison of Au, Ag, and Cu from Johnson and Christy [18] between 300 to 1,200 nm, **a** negative real part and **b** positive imaginary part

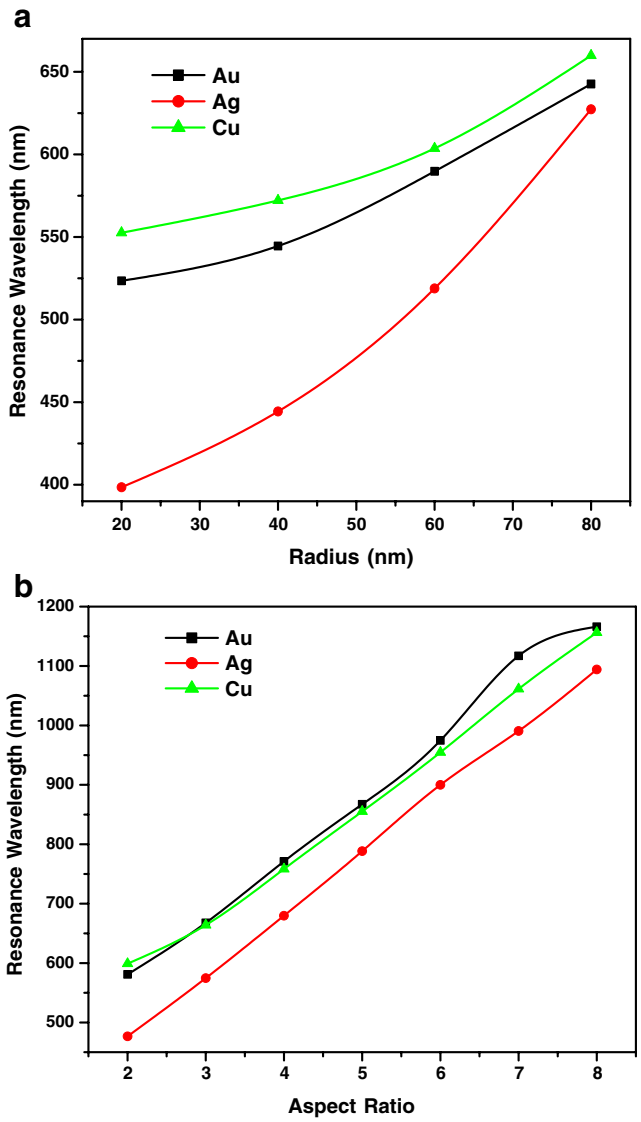

Fig. 2 Calculated LSPR wavelength of noble metal nanoparticles; **a** spherical nanoparticles with radius from 20 to 80 nm and **b** prolated shape nanoparticle from aspect ratios 2 to 8

Results and Discussion

Regarding the size and shape of nanoparticle, we first consider the sphere of radius (r) ranging from 20 to 80 nm. The simulation results are obtained by Mie Plot with different radius of sphere having medium like Au, Ag, and Cu and surrounding medium refractive index. The chosen surrounding mediums are water, ethanol, chloroform, and benzene with refractive indices 1.33, 1.36, 1.45, and 1.50, respectively. Simulation results show a red shift in LSPR with increase in the radius of sphere and its surrounding refractive index. This resonance condition for the LSPR is fulfilled if [3]

$$\varepsilon_1 = -\frac{1 - L_i}{L_i}\,\varepsilon_m \tag{8}$$

where, ε_1 is real part of dielectric constant of the material shown in Fig. 1 which is obtained from the experimental data [18] and L_i is the depolarization factor for a particular axis i of the prolate. The resonance wavelength can thus be determined from this condition. The value of "L_i=1/3" or less than "1/3" for spherical or prolate (depending on the aspect ratio) particles, respectively. The shift in LSPR with radius is exponential in nature and is shown in Fig. 2a. The exponential fit to the data is given by equation

$$\lambda_0 = y_0 + A\exp\left(\frac{r}{t}\right) \tag{9}$$

The constant y_0, A, and t are given in Table 1. The LSPR maxima is found in the order Cu>Au>Ag. In case of prolate, AR is varied from 2 to 8 by keeping the width fixed at 20 nm and altering the length in the steps of 20 nm in the same manner as in Becker et al. [10]. The increase in aspect ratio results a linear rise in the LSPR wavelength for all the three plasmonic materials as shown in Fig. 2b. The obtained linear fit equation is

$$\lambda_0 = x_0 + d \times \mathrm{AR} \tag{10}$$

The parameters x_0 and d are constants given in Table 2. The order of LSPR maxima for prolate nanoparticles shown in Fig. 2b is Au>Cu>Ag, whereas for aspect ratio 2 only, the order continues same as for spherical particle. The answerable parameter for initial mismatching is the real part of the dielectric constant of Au and Cu medium (Fig. 1a) because at this aspect ratio the LSPR position lies approximately below 600 nm for both, and in this region, the real part of dielectric function of Cu exhibits higher value than Au. Hence, the resonance condition described by Eq. 8 is satisfied at higher wavelength for Cu than Au.

With the increasing surrounding medium refractive index, we get the increased extinction cross section, and

Table 1 Values of parameters defined in Eq. 9 with errors indicated in parenthesis

Nanosphere medium	y_0	A	t	Regression coefficient	Chi-square
Au	465.02 (±36.94)	38.87 (±28.14)	52.51 (±18.26)	0.99696	25.42
Ag	305.81 (±10.31)	60.75 (±7.49)	47.49 (±2.70)	0.99991	2.77
Cu	526.77 (±2.60)	15.11 (±1.56)	36.78 (±1.45)	0.99993	0.46

Table 2 Values of parameters defined in Eq. 10 with errors indicated in parenthesis

Nanorod medium	x_0	d	Regression coefficient	Standard deviation
Au	367.48 (±19.49)	102.08 (±3.62)	0.99687	19.16
Cu	388.60 (±13.06)	95.10 (±2.42)	0.99838	12.83
Ag	267.73 (±5.62)	103.72 (±1.04)	0.99975	5.52

spectrum shifts toward higher wavelength region. Figure 3a shows the oscillation in refractive index sensitivity of different size nanosphere of Au, Ag, and Cu. The refractive index sensitivity of nanoparticles increases as the radius of particle increases. Interestingly, spherical particles over the whole range of the radius, studied here shows the index sensitivity order as Ag>Au>Cu. Hence, the use of plasmonic material towards the refractive sensing applications is useful in this order only for spherical nanostructures. The average refractive index sensitivities of Ag, Au, and Cu nanospheres are 237.18, 191.01, and 153.14 nm per refractive index unit (RIU), respectively.

In Fig. 3b, the refractive index sensitivity results are quite exciting. From aspect ratios 2 to 5, the order is Ag>Au>Cu; however, at aspect ratios 6, 7, and 8, the results are different. The average (for 2–8 aspect ratio range) refractive index sensitivities of Ag, Cu, and Au prolates are 530.97, 494.56, 448.68 nm/RIU, respectively. Hence, the observed variation in refractive index sensitivity order for noble metal nanoparticle geometry shows that the shape of nanoparticle plays a very crucial role in plasmonic index sensitivity. Plasmonic prolate exhibits two to three times higher sensitivity than the sphere.

The increasing size of the nanosphere or aspect ratio of the prolate increases the FWHM also, which may restrict the sensing resolution of plasmonic materials. For spherical particles, Fig. 4a illustrates the variation in FWHM. The FWHM (Γ) can be determined from [4]

$$\Gamma \approx 2\varepsilon_2 / \frac{\mathrm{d}\varepsilon_1}{\mathrm{d}\omega} \tag{11}$$

Equation 3 indicates that smaller the imaginary dielectric constant of the metal and steeper gradient of real part with frequency would give the narrow FWHM. The bulk dielectric function of Ag, Au, and Cu used in this calculation is obtained from the experimental data (http://philiplaven.com/MiePlot.htm) and is shown in Fig. 1. The imaginary part of Ag exhibits lower value over the entire visible to infrared region of EM spectrum as compared to Au and Cu (in Fig. 1a). Hence, from Eq. 3, it is understandable that Ag may exhibit narrower LSPR extinction spectrum.

In general, the trend in FWHM is in the order of Ag>Au>Cu. The importance of this statement may be considered, as the sensing resolution may be better for Cu in comparison to Au and Ag. These results are same as reported by Chan et al. [19] triangular metal nanoparticles. In Fig. 4b, the prolate experiences the order of FWHM over the entire range of aspect ratio as Cu>Au>Ag. To use these material nanoparticles as nanosensors, we need the separable LSPR peak with a slight change in the surrounding medium refractive index, which may be affected by FWHM.

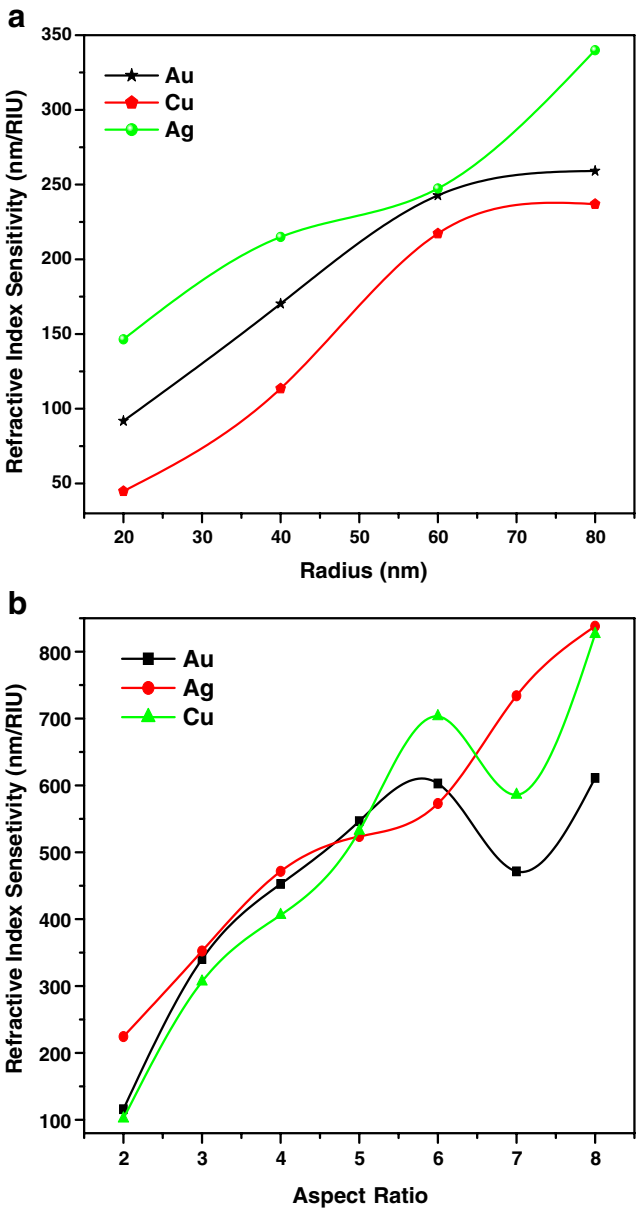

Fig. 3 Calculated refractive index sensitivity (S) of Au, Ag, and Cu; **a** spherical nanoparticles and **b** prolate shape

Therefore, the sensing figure of merit (FOM) is calculated as

$$\mathrm{FOM} = \frac{S\left(\frac{\mathrm{nm}}{\mathrm{RIU}}\right)}{\mathrm{FWHM(nm)}} \tag{12}$$

Fascinatingly, the order for FOM in spherical particles is Ag>Au>Cu. The optimized radius in this simulation is approximately 20 nm for Ag. Au shows the FOM maxima near 40-nm radius, whereas for Cu, the optimized radius lies between 40 to 60 nm. In general, Fig. 5a displays better FOM over the entire radius range of spheres for Ag. In average, the FOM for Ag, Au, and Cu nanospheres are 3.07, 1.02, and 0.86, respectively. Further, for aspect ratios 2, 3, 6, and 8, the FOM value is almost same for the Au and Cu prolates, i.e., at some aspect ratios, the plasmonic nanosensors made from Au and Cu show same sensing performance (Fig. 5b). However, FOM performance is better for Au at aspect ratios 4, 5, and 7 than Cu. Therefore, for prolate at a particular aspect ratio, Cu may be a better plasmonic material choice for sensing applications in comparison to Au due to its low cost. Ag prolate shows the better FOM performance over the whole range of aspect ratio except at 5. Thus, Ag prolate, in general, is much better than the gold because is exhibit larger FOM value in comparison to Au and is cheaper. In average, the FOM are 96.16, 15.64, and 7.12 for Ag, Au, and Cu, respectively. In general, Ag shows 6 and 14 times higher FOM performance in comparison to Au and Cu, respectively. Hence, in the case of spherical and prolate shaped particles, Ag exhibits much better FOM than Au and Cu if it can be protected from the oxidization.

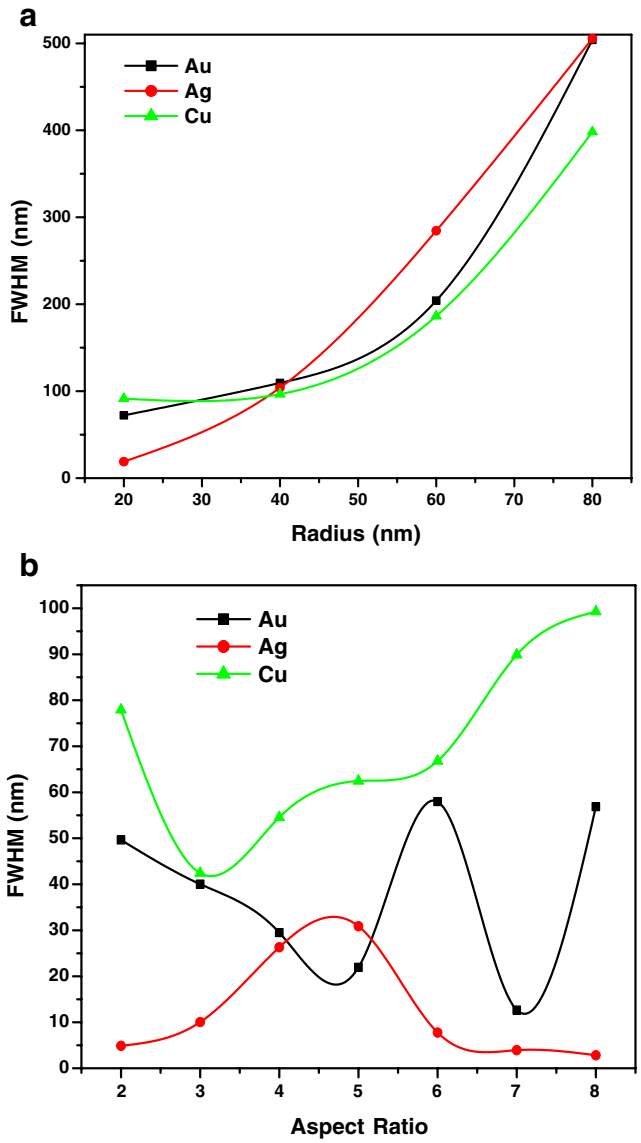

Fig. 4 FWHM **a** vs. radius of nanosphere and **b** vs. aspect ratio of prolate

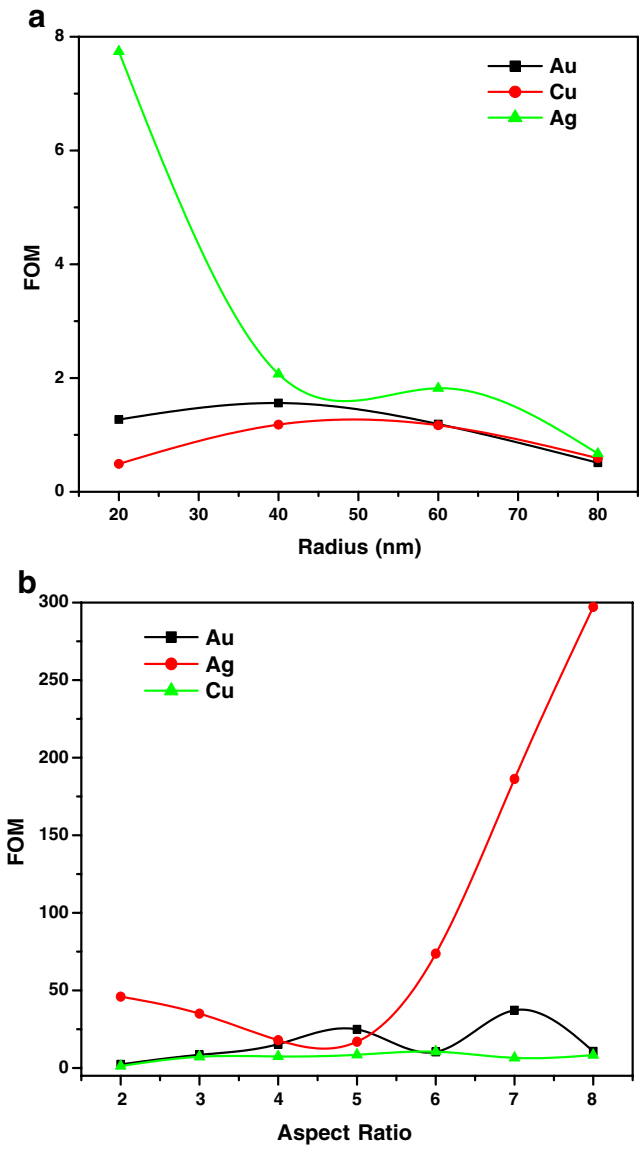

Fig. 5 Comparison of calculated FOM for noble metal nanoparticles; **a** nanosphere and **b** prolate

To understand the described sensing behavior of plasmonic nanoparticles, the quality factor [5, 10] defined as the resonance energy divided by the resonant line width has also been calculated. Figure 6a, b shows the quality factor variation with the size of nanosphere and aspect ratio of prolate, respectively. Evidently, there is a good similarity between the variation of FOM and quality factor with respect to both size and aspect ratio (Figs. 5 and 6). Hence, the key explanation for the sensing behavior is quality factor under the similar conditions. Thus, in quasi-static and electrodynamic studies [5], quality factor clearly explains the sensing behavior of noble metal nanoparticles. Fascinatingly, the Ag nanosphere exhibit higher FOM over the EM spectrum range of 400 to 600 nm (in Fig. 7a). The prolate shape of Ag shows higher FOM over the visible to infrared region of EM spectrum, (Fig. 7b) which is of particular interest for plasmonic sensing applications.

Conclusions

In conclusion, the plasmonic properties of noble metal nanoparticles (Au, Ag, and Cu) have been examined under quasi-static approximation. It is found that the LSPR of each metal particle is highly sensitive to even a small change in surrounding refractive index and that the shape of nanoparticle affects the sensitivity. Therefore, development of highly sensitive bio/chemo sensors based on plasmonic nanoparticles may be possible with due consideration given

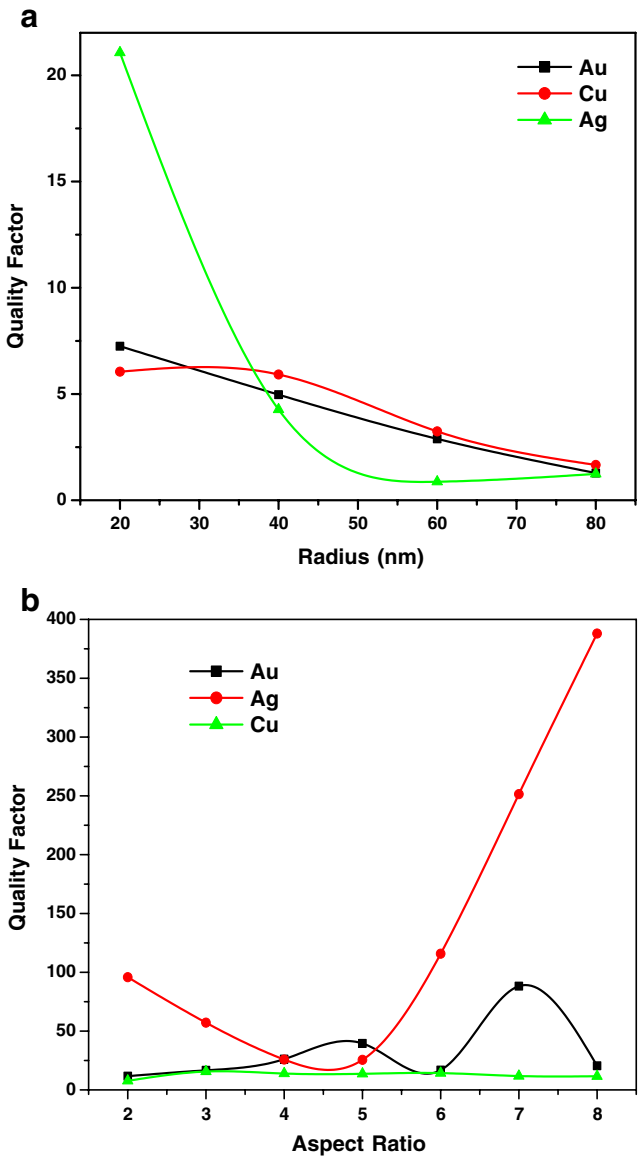

Fig. 6 The quality factor **a** vs. sphere radius of Ag, Au, and Cu and **b** vs. aspect ratio of Ag, Au, and Cu prolates

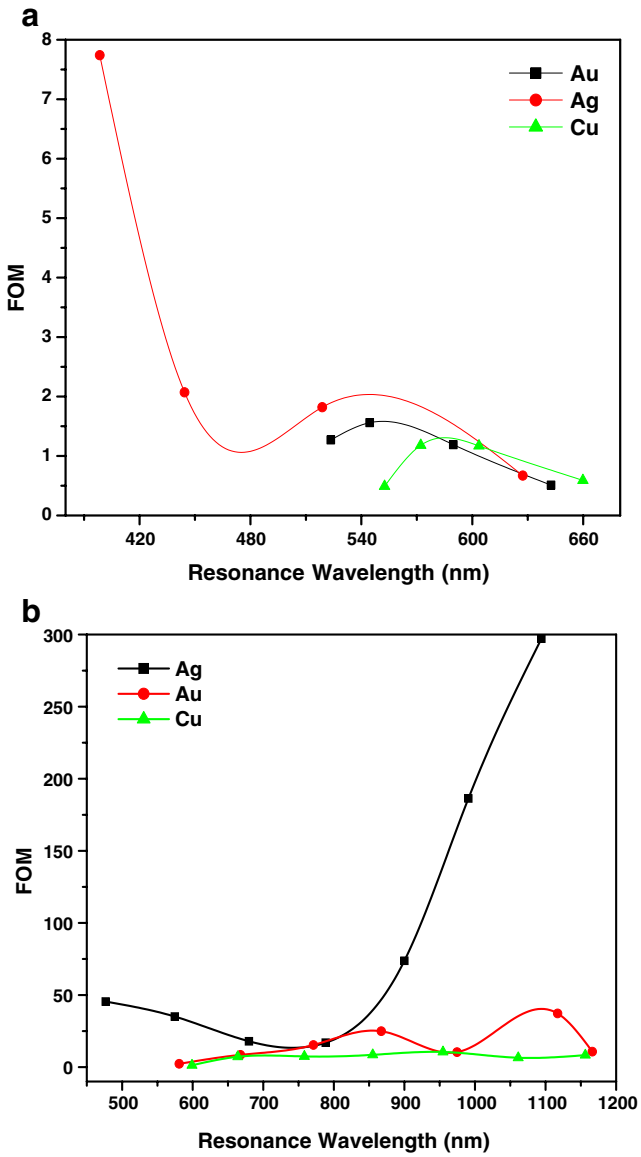

Fig. 7 FOM vs. resonance wavelength; **a** sphere and **b** prolate

to the particle shape and its material nature. From FOM viewpoint over the entire visible to infrared region of EM spectrum, the optimized material is Ag with its prolate shape.

References

1. Lal S, Link S, Halas NJ (2007) Nano-optics from sensing to waveguiding. Nat Photonics 1:641–648
2. Noguez C (2007) Surface plasmon on metal nanoparticles: the influence of shape and physical environment. J Phys Chem C 111:3806–3819
3. Link S, Mohamed MB, El-Sayed MA (1999) Simulation of the optical absorption spectra of gold nanorods as a function of their aspect ratio and the effect of the medium dielectric constant. J Phys Chem C 103:3073–3077
4. Lee K, El-Sayed M (2006) Gold and silver nanoparticles in sensing and imaging: sensitivity of plasmon response to size, shape, and metal composition. J Phys Chem B 110:19220–19225
5. Sekhon JS, Verma SS (2010) Optimal dimensions of gold nanorod for plasmonic nanosensors. Plasmonics. doi:10.1007/s11468-010-9182-3
6. Sherry LJ, Jin R, Mirkin CA, Schatz GC, Van Duyne RP (2006) Localized surface plasmon resonance spectroscopy of single silver triangular nanoprism. Nano Lett 6:2060–2065
7. Nehl CL, Liao H, Hafner JH (2006) Optical properties of star-shaped nanoparticles. Nano Lett 6:683–688
8. Jain PK, Lee KS, El-Sayed IH, El-Sayed MA (2006) Calculated absorption and scattering properties of gold nanoparticles of different size, shape, and composition: applications in biological imaging and biomedicine. J Phys Chem C 110:7238–7248
9. Cobley CM, Skrabalak SE, Campbell DJ, Xia Y (2009) Shape controlled synthesis of silver nanoparticles for plasmonic and sensing applications. Plasmonics 4:171–179
10. Becker J, Trugler A, Jakab A, Hohenester U, Sonnichsen C (2010) The optimal aspect ratio of gold nanorods for plasmonic bio-sensing. Plasmonics 5:161–167
11. Chan GH, Zhao J, Hicks EM, Schatz GC, Van Duyne RP (2007) Plasmonic properties of copper nanoparticles fabricated by nano-sphere lithography. Nano Lett 7:1947–1952
12. Chen H, Kou X, Yang Z, Ni W, Wang J (2008) Shape and size dependent refractive index sensitivity of gold nanoparticles. Langmuir 24:5233–5237
13. Chen H, Shao L, Woo KC, Ming T, Lin H, Wang J (2009) Shape-dependent refractive index sensitivity of gold nanocrystals with the same plasmon resonance wavelength. J Phys Chem C 113:17691–17696
14. Sarkar P, Bhui DK, Bar H, Sahoo GP, Samanta S, Pyne S, Misra A (2010) DDA-based simulation of uv-vis extinction spectra of Ag nanorod synthesized through seed-mediated growth process. Plasmonics. doi:10.1007/s11468-010-9167-2
15. Tilaki RM, Zad AI, Mahdavi SM (2007) Size, composition and optical properties of copper nanoparticles prepared by laser ablation in liquids. Appl Phys A 88:415–419
16. Liu CM, Guo L, Xu HB, Wu ZY, Weber J (2003) Seed-mediated growth and properties of copper nanoparticles, nanoparticle 1D arrays and nanorods. Microelectron Eng 66:107–114
17. Shrestha KM, Sorensen CM, Klabunde KJ (2010) Synthesis of CuO nanorods, reduction of CuO into Cu nanorods, and diffuse reflectance measurements of CuO and Cu nanomaterials in the near infrared region. J Phys Chem C 114:14368–14376
18. Johnson PB, Christy RW (1972) Optical constants of the noble metals. Phys Rev B 6:4370–4379
19. Chan GH, Zhao J, Schatz GC, Van Duyne RP (2008) Localized surface plasmon resonance spectroscopy of triangular aluminum nanoparticles. J Phys Chem C 112:13958–13963